Supporting Information for

Kinetics of the Oxidation of Phenols and Phenolic Endocrine Disruptors during Water Treatment with Ferrate (Fe(VI))

Yunho Lee[1,2], Jeyong Yoon[*1], and Urs von Gunten[**2]

[1]*School of Chemical and Biological Engineering, College of Engineering, Seoul National University, San 56-1, Sillim-dong, Gwanak-gu, 151-742 Seoul, Korea*

[2]*Swiss Federal Institute for Aquatic Science and Technology, EAWAG, 8600 Dübendorf, Switzerland*

Submitted to

Environmental Science & Technology

*[1]Corresponding author, e-mail: jeyong@snu.ac.kr, phone: +82-02-880-8927; fax: +82-02-876-8911

**[2]Co-corresponding author, e-mail: vongunten@eawag.ch, phone: +41-1-823-5270; fax: +41-1-823-5028

This document was prepared on 13th, September, 2005, as a Supporting Information of ES05 1198w, consisted of 14 pages including 10 texts and 6 figures.

Text S1. Structures of Selected Phenolic EDCs.

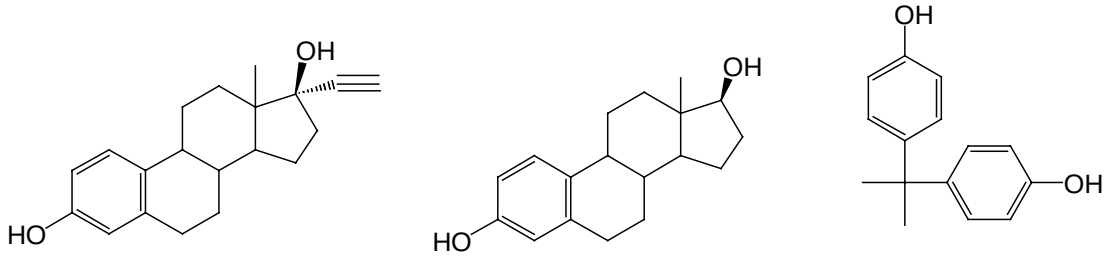

17α-ethinylestradiol (EE2) **β-estradiol (E2)** **Bisphenol-A (BPA)**

Figure S1. Structures of the selected phenolic EDCs, 17α-ethinylestradiol (EE2), 17β-estradiol (E2), and bisphenol-A (BPA).

Text S2. Phenolic EDCs Determination by HPLC Method.

EE2, E2, and BPA were determined using high-performance liquid chromatography (HPLC, Hewlett-Packard, 1050 series) with a fluorescence detector (HP 1064A)A C-18 reverse phase column (Nucleosil 100, 5-μm, Machery-Nagel) was used as the stationary phase with 0.6 mL min^{-1} of the eluent consisting of 50% acetonitrile and 50% 10 mM phosphoric acid. An excitation wavelength of 229 nm and an emission wavelength of 309 nm were used to detect the fluorescence. The detection limits were ~ 5 nM for all three phenolic EDCs (EE2, E2, and BPA) for an injection volume of 100 μL. The 95% confidence interval for a single measurement was typically ± 5%.

Text S3. Order of Reaction between Fe(VI) and Phenol.

The general rate expression for the reaction between Fe(VI) and phenol (PhOH) can be written as

$$-d[Fe(VI)_T]/dt = k_{app}[Fe(VI)]_{tot}^{a}\,[PhOH]_{tot}^{b} \quad (1)$$

where $[Fe(VI)]_{tot}$ and $[PhOH]_{tot}$ are the molar concentrations of the total Fe(VI) ($H_nFeO_4^{n-2}$) and PhOH species (PhOH/PhO^-), respectively; a and b are the orders of the reaction; k_{app} is the apparent rate constant of the reaction between Fe(VI) and PhOH.

The kinetic experiments were undertaken under pseudo-first-order conditions for Fe(VI), where an excess of PhOH was used ($[Fe(VI)]_{tot}$ < 2 μM and $[PhOH]_{tot}$ > 50 μM). Under these conditions, eq 1 can be rewritten as

$$-d[Fe(VI)]_{tot}/dt = k' [Fe(VI)]_{tot}^{a} \quad (2)$$

where $k' = k_{app} [PhOH]_{tot}^{b}$

The pseudo-first-order rate constants for the decrease of Fe(VI) (k′) were obtained by measuring the decrease of Fe(VI) concentration as a function of time in the presence of excess PhOH. Figure S2, as representative data at $[PhOH]_{tot}$ = 500 μM and pH = 9.0 (25 mM phosphate/5 mM borate buffer), shows that Fe(VI) follows a pseudo-first order decrease (R^2 > 0.99) with a rate constant of 1.6×10^{-2} s^{-1}, confirming that the reaction is first-order with respect to Fe(VI) (a = 1). Then, k′ values were determined at various concentrations of PhOH (50–500 μM) at pH = 9.0. In all cases, the decrease of Fe(VI) was confirmed to be first-order with respect to Fe(VI) (R^2 > 0.99). Figure S3 clearly shows the linearity of k′ with respect to $[PhOH]_{tot}$ (R^2 > 0.99), confirming this reaction to also be first-order with respect to PhOH (b = 1). From the slope in Fig. S3, the apparent second-order rate constant for the reaction between Fe(VI) and PhOH, $k_{app} = 3.2\times10^{1}$ $M^{-1}s^{-1}$ was obtained at pH 9.0.

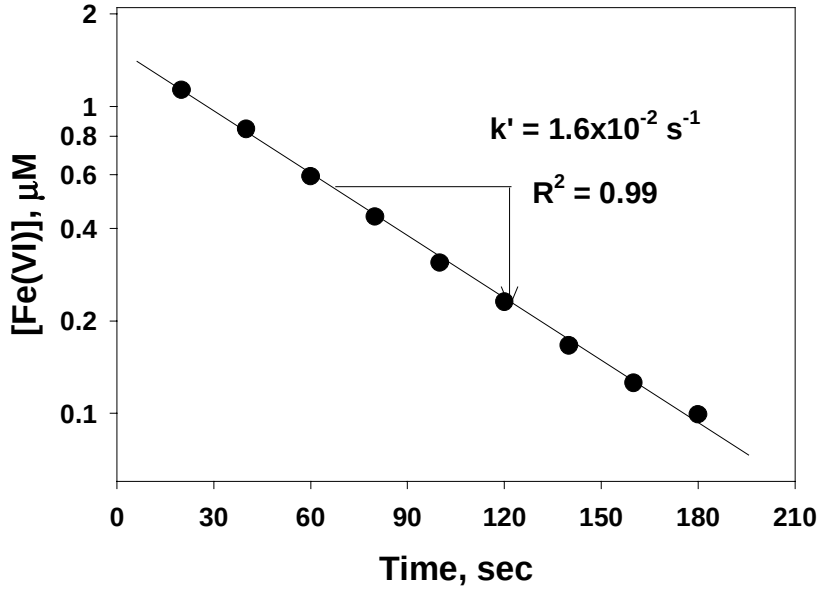

Figure S2. Pseudo-first-order kinetic plot of the consumption of Fe(VI) by excess PhOH (500 µM) at pH 9.0 and 25°C.

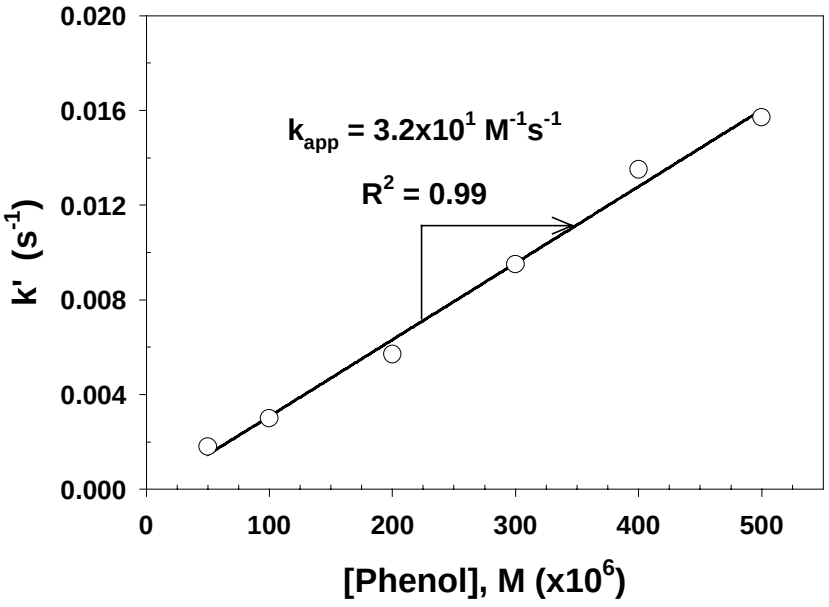

Figure S3. Plot of the pseudo-first-order rate constant for the decrease of Fe(VI) (k′) vs initial PhOH concentration at pH 9.0 and 25°C.

Text S4. Determination of second-order rate constant.

1) Phenolic EDCs (EE2, E2, and BPA).

The apparent second-order rate constants for the selected phenolic EDCs (EE2, E2, and BPA) were determined by monitoring their decrease in the presence of at least a 10 fold excess of Fe(VI). A 250 mL glass bottle with a dispenser system mounted onto the screwtop was used as a reactor. The kinetic runs were begun by adding 5–10 mL of the Fe(VI) stock solution to a solution containing each phenolic EDC (0.25 μM), yielding an initial Fe(VI) concentration of 4–10 μM. The first sample (5 mL) was withdrawn after 20 sec using the dispenser system. Subsequently, 7 more samples were withdrawn at set time intervals ranging from 40 sec to 20 min depending on the apparent oxidation rate of the phenolic EDCs. In addition, it was necessary to measure the rate of Fe(VI) decrease because Fe(VI) is unstable at pH < 8 (*1*). For this, 3 to 7 samples were collected for the Fe(VI) analysis using the ABTS method. For phenolic EDCs analysis by the HPLC method, the Fe(VI) residuals were immediately quenched by mixing the sample with 0.1 mL ascorbic acid (25 mM). Ascorbic acid reacts rapidly with Fe(VI) (second-order rate constants are above 10^6 $M^{-1}s^{-1}$ at pHs 6.8–11.5 ranges) (*2*) and are found to be a good quenching reagent for Fe(VI). In addition, reduction of oxidation products to parent EDCs by ascorbic acid was not observed within several days after quenching process. Sample analysis by the HPLC methods were conducted within a few hours after sampling. The data was evaluated by plotting the natural logarithm of the phenolic EDCs concentration versus the Fe(VI) exposure, i.e., Fe(VI) concentration integrated over time, as shown in eq 3.

$$\ln([EDC]/[EDC]_0) = -k_{app} \int_0^t [Fe(VI)]\,dt \qquad (3)$$

where the term $\int_0^t [\mathrm{Fe(VI)}]\,dt$ represents the Fe(VI) exposure, the time integrated concentration of Fe(VI) and k_{app} (the slope of resulting straight line) represents the apparent second-order rate constant.

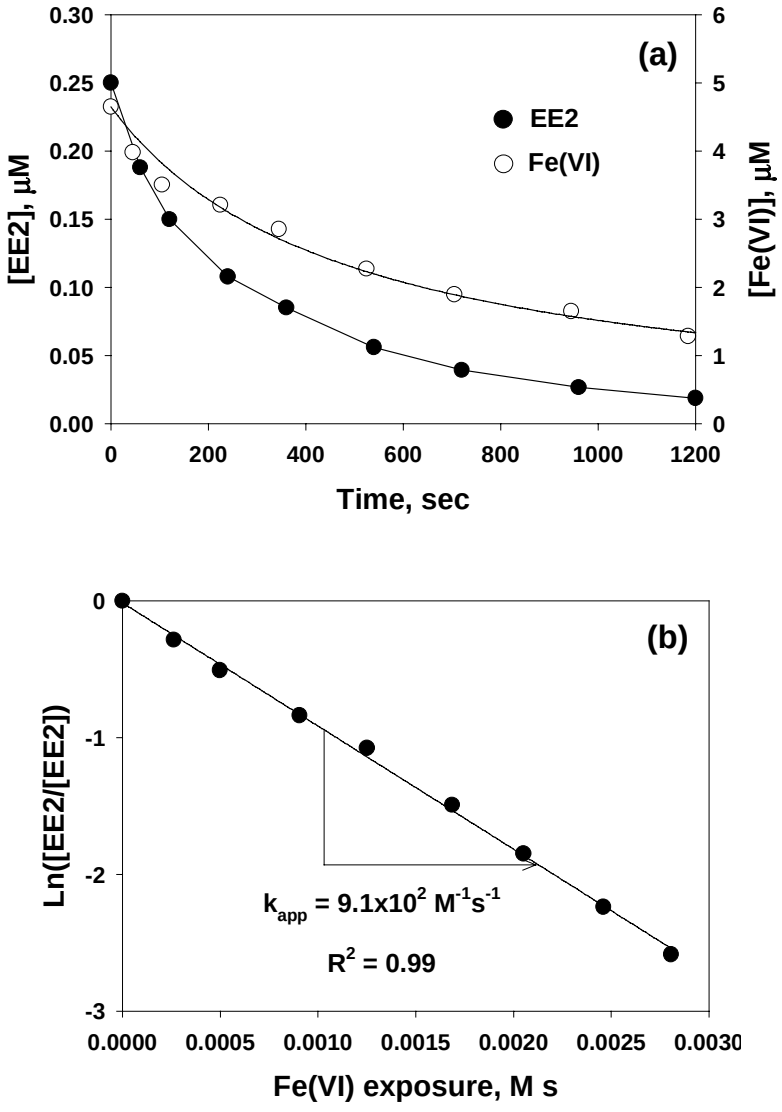

Figure S4. (a) Concentration time profiles of EE2 and Fe(VI). $[EE2]_0$ = 0.25 μM, $[Fe(VI)]_0$ = 4.7 μM, pH = 6 (25 mM phosphate buffer), and 25°C, (b) fit of EE2 oxidation by Fe(VI) with second-order reaction kinetics (eq 3).

Figure S4a shows the concentration time profiles of EE2 and Fe(VI) during the oxidation of EE2 (0.25 μM) by excess Fe(VI) (4.7 μM) at pH 6 as a representative data. As expected, Fe(VI) was unstable at pH 6 and about 70% of initial Fe(VI) decayed within 20 min of reaction time. Nonetheless, the Fe(VI) concentration was always in excess to the concentration of EE2 within the studied reaction time ([EE2] << [Fe(VI)]). Figure S4b clearly shows that eq 3 successfully represents the kinetic of EE2 removal by Fe(VI) oxidation ($R^2 > 0.99$). From the slope of the curve in Fig. S4b, the apparent second-order rate constant of EE2 oxidation by Fe(VI) was determined as $k_{app} = 9.1\times10^2\ M^{-1}s^{-1}$ at pH 6 and 25°C.

2) Substituted Phenols.

The apparent second-order rate constants for the substituted phenols were determined under the conditions with the substituted phenols in excess. In this case, the decrease in the Fe(VI) concentration was monitored instead of the disappearance of the target compound. The kinetic runs were started by adding 5 mL of the Fe(VI) stock solution to the solution containing each substituted phenol (250 mL), yielding an initial Fe(VI) concentration of 0.5–2.0 μM. The Fe(VI) decrease was monitored using the ABTS method. At these low initial Fe(VI) concentrations (0.5–2.0 μM), the self-decay of Fe(VI) was negligible compared with Fe(VI) decay as a result of its reaction with the substituted phenols. The preliminary experiments showed that the self-decay of Fe(VI) was < 5% within 3 min at an initial Fe(VI) concentration of 1 μM and at pH 6 (data not shown). The data was evaluated by plotting the natural logarithm of the Fe(VI) concentration versus the reaction time. The slope of the resulting straight line represents the pseudo-first-order rate constant. The apparent second-order rate constant was obtained by dividing the pseudo-first-order rate constant by the concentration of the substituted phenols.

Text S5. Lake Zürich Water and Kloten Wastewater.

Lake Zürich water was taken from a depth of 30 m below the surface. Lake Zürich is a deep oligotrophic, seasonally stratified lake with an alpine catchment area. In the conventional activated sludge treatment (CAS) plant in Kloten, the combined sewage of 55,000 population equivalents is treated using a conventional activated sludge system that is equipped with a primary clarifier, nitrification, and denitrification (11 ± 2 days sludge age). The waters were filtered (0.45 μm cellulose nitrate) upon arrival and stored at 4°C until use

Text S6. Critical Evaluation of the Contributions of each Fe(VI) and phenolic EDC species to the Overall Reaction.

The reactions of H_2FeO_4 and FeO_4^{2-} with the phenolic EDCs were neglected in the model calculations due to the following reasons. First, the reactions between H_2FeO_4 and the phenolic EDCs were neglected because the abundance of H_2FeO_4 is rather low within the pH range studied ($pK_{a,H2FeO4}$ is 3.5, which is 2.5 pH units lower than the lowest pH value studied). Second, the reactions between FeO_4^{2-} and the phenolic EDCs were neglected based on the following observation. The k_{app} decreased with decreasing $HFeO_4^-$ concentration with increasing pH (See Figure 1 in the main text). This suggests that the overall reactions may be dominated by the reactions involving $HFeO_4^-$, and that FeO_4^{2-} does not make a significant contribution to the overall reactivity of the phenolic EDCs with Fe(VI). Similar observations, i.e. $HFeO_4^-$ rather than FeO_4^{2-} represents the primary oxidant species in the Fe(VI) reactions, have been reported (*1, 3, 4*).

Regression analysis of the experimental data with the general model, eq 2 (in the main text), was performed to test above assumption that of the three Fe(VI) species, only $HFeO_4^-$

contributes significantly to the overall reaction between Fe(VI) and phenolic EDCs. This regression yielded values close to zero for the rate constants k_{ij} corresponding to the reactions omitted from the simplified models (reactions of H_2FeO_4 and FeO_4^{2-}). The exclusion of these values did not significantly affect the model accuracy. This provides additional support for the assumptions made in the model.

Text S7. Ionization Fraction of Fe(VI) and Phenolic Compounds (α_i and β_j).

The values of α_i and β_j can be expressed using the equilibrium constants of Fe(VI) ($K_{a,\ H2FeO4}$ = 3.50 and $K_{a,\ HFeO4-}$ = 7.23) and the corresponding phenolic compounds as shown below.

1) Ionization fraction of Fe(VI) species

$$\alpha_1 = \frac{[H_2FeO_4]}{[Fe(VI)]_t} = \frac{[H^+]^2}{T_1},\ \alpha_2 = \frac{[HFeO_4^-]}{[Fe(VI)]_t} = \frac{[H^+]K_{a,H2FeO4}}{T_1},\ \alpha_3 = \frac{[FeO_4^{2-}]}{[Fe(VI)]_t} = \frac{K_{a,H2FeO4}K_{a,HFeO4-}}{T_1},\ \text{and}$$

$T_1 = [H^+]^2 + [H^+]K_{a,H2FeO4} + K_{a,H2FeO4}K_{a,HFeO4-}$

2) Ionization fraction of phenolic compounds of monoprotic acids ($K_{a,\ PhOH}$): EE2, E2, and all substituted phenols in Table 1)

$$\beta_1 = \frac{[PhOH]}{[PhOH]_t} = \frac{[H^+]}{[H^+] + K_{a,\ PhOH}},\ \beta_2 = \frac{[PhO^-]}{[PhOH]_t} = \frac{K_{a,PhOH}}{[H^+] + K_{a,PhOH}}$$

3) Ionization fraction of phenolic compounds of diprotic acids ($K_{a,\ PhOH}$ and $K_{a,\ PhO-}$): BPA

$$\beta_1 = \frac{[PhOH]}{[PhOH]_t} = \frac{[H^+]^2}{T_2},\ \beta_2 = \frac{[PhO^-]}{[PhOH]_t} = \frac{[H^+]K_{a,PhOH}}{T_2},\ \beta_3 = \frac{[PhO^{2-}]}{[PhOH]_t} = \frac{K_{a,PhOH}K_{a,PhO-}}{T_2},\ \text{and}\ T_2 =$$

$[H^+]^2 + [H^+]K_{a,PhOH} + K_{a,PhOH}K_{a,PhO-}$

Text S8. Determination of k_{ij} Values by Least Square Regression Analysis.

The specific second-order rate constants, k_{ij}, and the standard errors were determined by a nonlinear least squares regression of the experimental k_{app} data. The regression was performed using the regression function in Microsoft Excel 2002 software. In the regression analysis, eq 6 (main text) was used for EE2 and E2 and eq 7 (main text) was used for BPA.

Text S9. Linear Free Energy Relationships

1) σ Constant.

Hammett-type correlations ($\log k = \log k_0 + \rho\sigma$) were tested for both k_{21} and k_{22} (*See Table 1, main text*) vs three sets of σ constants, σ^+, σ, and σ^- (*5*). The obtained correlation equations are as follows:

$$\log(k_{21}) = 2.24\ (\pm0.05) - 2.27\ (\pm0.17)\sigma^+ \qquad r^2 = 0.974,\ n = 7 \qquad (4)$$

$$\log(k_{22}) = 4.33\ (\pm0.08) - 3.60\ (\pm0.18)\sigma^+ \qquad r^2 = 0.983,\ n = 9 \qquad (5)$$

$$\log(k_{21}) = 2.41\ (\pm0.14) - 2.99\ (\pm0.51)\sigma \qquad r^2 = 0.852,\ n = 8 \qquad (6)$$

$$\log(k_{22}) = 4.66\ (\pm0.16) - 4.30\ (\pm0.38)\sigma \qquad r^2 = 0.940,\ n = 10 \qquad (7)$$

$$\log(k_{21}) = 2.46\ (\pm0.10) - 2.97\ (\pm0.34)\sigma^- \qquad r^2 = 0.927,\ n = 8 \qquad (8)$$

$$\log(k_{22}) = 4.72\ (\pm0.17) - 3.09\ (\pm0.29)\sigma^- \qquad r^2 = 0.935,\ n = 10 \qquad (9)$$

2) pK_a values.

Figure S5 shows good linear relationships for both k_{21} and k_{22} vs pK_a values (*See Table 1,*

main text). The obtained correlation equations are as shown in eqs 10 and 11.

$$\log(k_{21}) = -11.57\ (\pm 2.02) + 1.42\ (\pm 0.21)pK_a \qquad r^2 = 0.886,\ n = 8 \qquad (10)$$

$$\log(k_{22}) = -9.62\ (\pm 1.45) + 1.45\ (\pm 0.16)\ pK_a \qquad r^2 = 0.916,\ n = 10 \qquad (11)$$

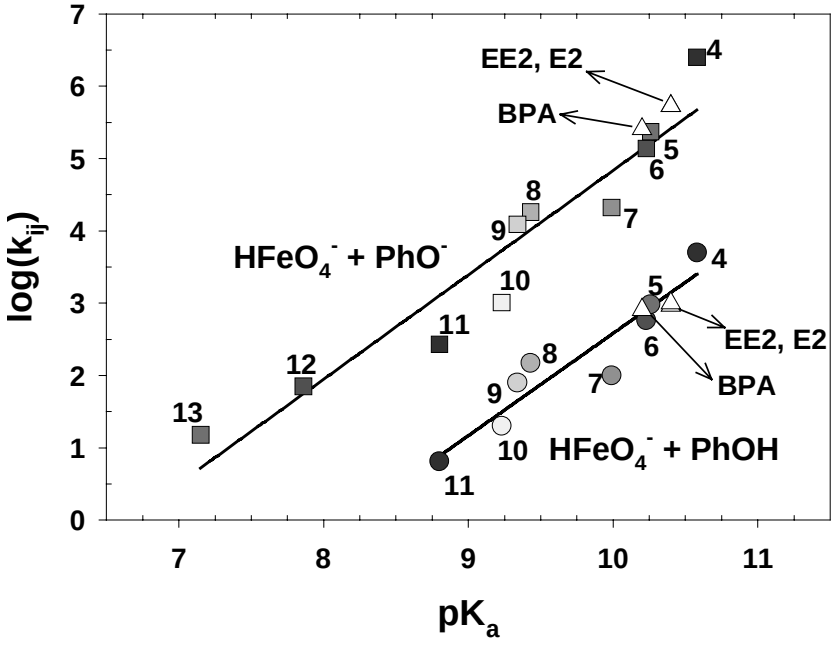

Figure S5. Correlations between the second-order rate constants of the reactions between $HFeO_4^-$ with the undissociated phenols (k_{21}) and the dissociated phenols (k_{22}) vs pK_a values. The numbers of the compounds correspond to those in Table 1 (main text).

If eqs 10 and 11 are used to predict the rate constant of the oxidation of the phenolic compounds by Fe(VI), the following two points should be considered. Firstly, the rate constant for the phenolic compounds with pK_a values are < ~7.9 can be higher than that predicted using eqs 10 and 11. This is because the reaction between H_2FeO_4 and the dissociated phenol can

contribute significantly to the overall reaction. This phenomenon was observed for 4-cyanophenol and 4-nitrophenol with pK_a values of 7.86 and 7.15, respectively. Secondly, the rate constant predicted using eqs 10 and 11 can differ slightly from the rate constant of phenolic compounds oxidation by Fe(VI) by the stoichiometric factor (η). The value of η can deviate from 1 as a result of fast side reactions of Fe(VI) with the products of the primary reactions. Nevertheless, the values of η for the reaction between the substituted phenols and Fe(VI) are not expected to significantly deviate from 1 based on the reaction scheme proposed for phenol oxidation by Fe(VI) (*6*, *7*). Figure S5 also shows that the plots of k_{21} and k_{22} of EE2, E2, and BPA vs their pK_a are in line with the correlation eqs 10 and 11, respectively. This highlights the success of using eqs 10 and 11 to predict the rate constants of phenolic compounds oxidation by Fe(VI).

3) Estimation of σ^+,σ, and σ^- constants of EE2, E2, and BPA

The σ^+, σ, and σ^- constants of EE2, E2, and BPA are not available in the literatures. Since these phenolic EDCs are of great concern in aquatic environments, and in addition they can be readily transformed by several water treatment oxidants, it will be useful to know their σ^+, σ, and σ^- constants to predict their oxidation rates during water treatment by oxidation. The σ^+, σ, and σ^- constants of EE2, E2, and BPA are estimated by using eqs 4–9 and the corresponding k_{ij} values (k_{21} and k_{22} in Table 1, main text) determined this study. The values are as follows.

EE2: $\sigma^+ = -0.36$, $\sigma = -0.22$, $\sigma^- = -0.25$

E2: $\sigma^+ = -0.36$, $\sigma = -0.22$, $\sigma^- = -0.25$

BPA: $\sigma^+ = -0.23$, $\sigma = -0.11$, $\sigma^- = -0.11$

Text S10. Oxidation Kinetics of BPA in Natural Water and Wastewater.

Lake Zurich water and Kloten wastewater were spiked with 0.15 μM BPA and treated with Fe(VI) at a dose of 6 and 20 μM, respectively. Figure S6 shows the time-dependent concentrations of EE2 and Fe(VI) during treatment of Lake Zurich water (Fig. S6a) and Kloten wastewater (Fig. S6b), respectively. In addition, Figure S6 shows that the determined rate constants ($k_{Fe(VI)}$) can be applied to predict BPA removal kinetics in real waters.

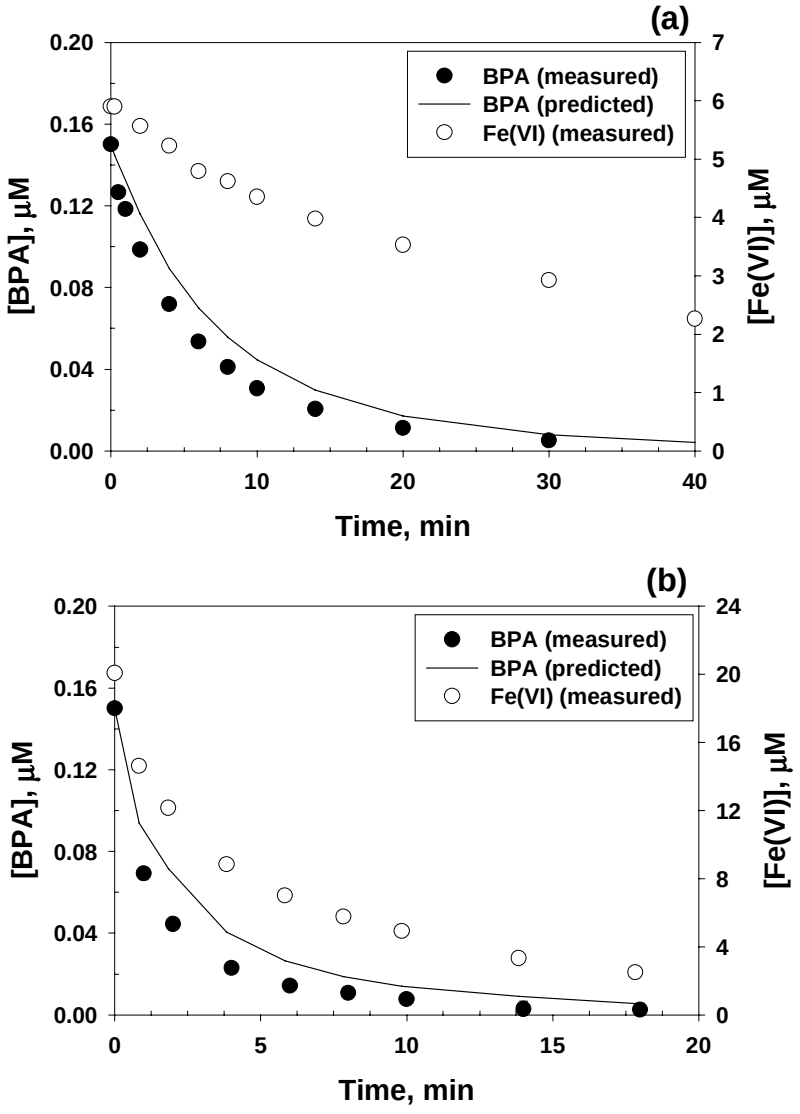

Figure S6. Oxidation kinetics of BPA by Fe(VI) during treatment of (a) lake water and (b)

wastewater. Symbols represent measured data, and solid lines represent model prediction. Experimental conditions: pH = 8 and T = 25°C.

Literature Cited

(1) Rush, J. D.; Zhao, Z.; Bielski, B. H. J. Reaction of ferrate(VI)/ferrate(V) with hydrogen peroxide and superoxide anion–a stopped-flow and premix pulse radiolysis study. *Free Rad. Res.* **1996**, *24*, 187–198.

(2) Cyr, J. E.; Bielski, B. H. J. The reduction of ferrate(VI) to ferrate(V) by ascorbate. *Free. Rad. Biol. Med.* **1991**, 157–160.

(3) Huang, H.; Sommerfeld, D.; Dunn, B. C.; Lloyd, C. R.; Eyring, E. M. Ferrate(VI) oxidation of aniline. *J. Chem. Soc. Dalton Trans.* **2001**, 1301–1305.

(4) Sharma, V. K.; Burnett, C. R.; O'Connor, D. B; Cabelli, D. Iron(VI) and iron(V) oxidation of thiocyanante. *Environ. Sci. Technol.* **2002**, *36*, 4182–4186.

(5) Hansch C.; Leo, A.; Taft, R. W. A survey of Hammett substutient constants and resonance and field parameters. *Chem. Rev*. **1991**, *91*, 165–195.

(6) Rush, J. D.; Cyr, J. E.; Zhao, Z.; Bielski, B. H. J. The oxidation of phenol by ferrate(VI) and ferrate(V). A pulse radiolysis and stopped-flow study. *Free Rad. Res.* **1995**, *22*, 349–360.

(7) Huang, H.; Sommerfeld, D.; Dunn, B. C.; Eyring, E. M.; Lloyd, C. R. Ferrate(VI) oxidation of aqueous phenol: Kinetics and mechanism. *J. Phys. Chem. A.* **2001**, *105*, 3536–3541.